

Biogenic Synthesis of Selenium Nanoparticles using *Diospyros montana* Bark Extract: Characterization, Antioxidant, Antibacterial, and Antiproliferative Activity

Abhijeet Puri* and Swati Patil

Department of Pharmacognosy, K M Kundnani College of Pharmacy,
Cuffe Parade, Mumbai-400005 (M.S.) India.

<http://dx.doi.org/10.13005/bbra/2997>

(Received: 01 April 2022; accepted: 30 June 2022)

Selenium nanomaterials (Nano-Se) are new selenium sources with excellent biocompatibility, degradability, and bioactivities. The objective of the present study is the green synthesis of selenium nanoparticles (SeNPs) using *Diospyros montana* Roxb (DM) bark extract, its characterization, and evaluation for in-vitro antioxidant, antibacterial and anticancer activities. To synthesize *Diospyros montana*- selenium nanoparticles (DM-SeNPs), selenious acid (H₂SeO₃) was reduced using *D. montana* extract via precipitation technique. UV-Vis, FTIR, XRD, SEM, EDAX, and ICP-AES were used to characterize DM-SeNPs. The DPPH free radical scavenging assay and reducing power capacity were used to test DM-SeNP for antioxidant activity. The antibacterial properties of the DM-SeNP were tested using the well diffusion method against gram-positive and gram-negative microorganisms. DM-SeNPs were also subjected to antiproliferative activity using MTT assay via MCF-7 cell line. A peak in UV at 289 nm validated the synthesis of DM-SeNPs. According to DLS, SEM, and TEM images, the size of DM-SeNPs was between 100-150 nm. XRD analysis confirmed the crystallinity of DM-SeNPs. Selenium was verified in colloidal dispersion using EDAX analysis, and ICP-AES confirmed selenium content $63.45 \pm 18.3 \mu\text{g/mL}$ in DM-SeNP. The IC₅₀ $24.72 \pm 0.63 \mu\text{g/mL}$ and EC₅₀ $46.30 \pm 0.21 \mu\text{g/mL}$ values indicated that the DM-SeNPs had a good antioxidant capacity. DM-SeNPs showed comparative better antibacterial potential. The inhibition zones were found to be the highest for *E. coli* (48.00 mm), *B. subtilis* (44.14 mm), *Klebsiella pneumonia* (36.20 mm), and *S. aureus* (34.16mm), respectively. Antiproliferative activity was carried out, which showed DM-SeNPs were cytotoxic to breast cancer cells line (MCF-7). The IC₅₀ values for DM-SeNPs were found to be $38.19 \pm 0.27 \mu\text{g/mL}$ and Doxorubicin $6.41 \pm 0.09 \mu\text{g/mL}$, respectively. The study suggests that DM-SeNPs display moderate cytotoxicity that could dose-dependently inhibit cell proliferation. Thus, experimental evidence provides insight into selenium nanoparticle synthesis, its potential therapeutic value, and the prospect of developing a formulation containing DM-SeNPs.

Keywords: Antioxidant; Antibacterial; Antiproliferative activity;
Diospyros montana; Green Synthesis; Selenium nanoparticles.

Nanotechnology has evolved into a promising technology in the twenty-first century, allowing the fabrication of nanoscale structures with superior capabilities¹. These size-dependent

capabilities give nanostructures an advantage over bulky materials in catalysis, electronics, biomedical, therapeutics, and biosensing². Nanoparticles have been the focal point of attention

*Corresponding author E-mail: abhijeetp@sjipr.edu.in

in therapeutics and medicine, owing to rapid advances in nanotechnology³; Nanomedicine is a term that describes the usage of nanotechnology in disease detection, diagnosis, and treatment. This new field has shown the revolutionary potential of current diagnostics and treatment practices^{4, 5}. Green nanotechnology aims for a broad range of scientific goods and processes that are highly safe, energy-efficient, waste-free, and significantly reduce greenhouse gas emissions⁶. Green source-mediated synthesis allows for finely controlled nanoparticle size and shape, as plants serve as stabilizing and reducing agents⁷. Additionally, the therapeutic effect of biogenic nanoparticles is more significant than that of chemically produced nanoparticles^{8, 9}.

Selenium nanomaterials (Nano-Se) are new selenium sources with superior *in-vivo* bioavailability while minimizing the risk of selenium toxicity¹⁰. Selenium nanoparticles (SeNPs) have shown much more excellent biocompatibility and degradability *in-vivo* than metals of great worth, such as silver, gold, and platinum. Se in various nanoforms has also shown lesser toxicity and higher antioxidant and antitumor potential than organic and inorganic selenium types^{11, 12}. The activity of glutathione peroxidase (GSH-Px) and thioredoxin reductase is increased by nano-selenium with low toxicity and high antioxidant activity. As a result, nanoparticles may be helpful because the nanoparticle size affects biological activity^{13, 14}. Size-dependent binding of free radicals is possible with SeNPs varying in size from 5 to 200 nm. Chemical reduction is the most prevalent method for obtaining selenium nanoparticles in various ways¹⁵. In the fabrication of SeNPs, the green chemistry of synthetic methodologies using biological processes such as enzymes, microbes, and plant extracts plays a vital role¹⁶. Phytoextracts in the fabrication of SeNPs are the most environmentally friendly alternative to the current chemical and physical methods¹⁷. This technique is applied to reduce toxicity and generate green chemistry. The principal phytochemicals utilized to fabricate SeNPs are flavonoids, tannins, aldehydes, ketones, terpenoids, carboxylic acids, alkaloids, and quinones. The fast conversion of selenium ions to SeNPs is caused by reducing water-soluble phytochemicals like flavones, tannins, quinones, and organic acids¹⁸.

Diospyros montana Roxb. (*D. montana*) is a member of the Ebenaceae family¹⁹. The phytochemical analysis of *D. montana* bark extract revealed the presence of steroids, naphthoquinones, triterpenes, polyphenols, and flavonoids²⁰. In the past, the *D. montana* plant has been utilized as an anti-inflammatory, antiviral, anticancer, inhibitor of prostaglandin production, hypolipidemic, and antileukemic agent²¹. *D. montana* bark extract contains a bisnaphthoquinonoid compound called diospyrin, which serves as a tumor inhibitor²². *D. montana* is a suitable plant for the green synthesis of SeNPs due to its potential components²³. As a result, this research is projected to rationalize the fabrication of DM-SeNPs using phytoconstituents from *D. montana* bark extract. Thus, it was hypothesized to synthesize the *Diospyros montana*- selenium nanoparticles DM-SeNPs and characterize them using various techniques, including Ultraviolet-visible spectroscopy (UV), Fourier-transform infrared spectroscopy (FT-IR), Scanning electron microscope (SEM), Dynamic Light Scattering (DLS), Zeta Potential (ZP), X-ray diffraction (XRD), Energy-dispersive X-ray analysis (EDX), Transmission Electron Microscopy (TEM), and Inductively coupled plasma atomic emission spectroscopy (ICP-AES). Further, these fabricated SeNPs have also been studied for antioxidant, antimicrobial, and anticancer activity.

MATERIALS AND METHOD

Chemicals and Reagents

Selenious acid (H₂SeO₃) was procured from Sigma-Aldrich Chemicals, India. The 2,2-diphenyl-1-picryl hydrazyl (DPPH), gallic acid, phenol reagent (Folin & Ciocalteu's), sodium nitrate, aluminum chloride, sodium carbonate, trichloroacetic acid, ferric chloride, and potassium ferricyanide were acquired from Loba Chemicals in India. Throughout the experiment, deionized and sterile distilled water only was used. All the remaining compounds in this analysis were of analytical grade.

Plant collection and authentication

Fresh *D. montana* bark was collected from Palghar's local contentment area. Dr. Jayananda Tosh, Senior Botanist, Research Guide SDSMS, College, Palghar, identified and authenticated the

plant sample. A sample specimen (V.C./154/2019-20) is deposited in the Pharmacognosy Department at Principal K. M. Kundnani College of Pharmacy, Mumbai, Maharashtra.

EXPERIMENTAL

Plant Extract Preparation and Qualitative Phytochemical Screening

To eliminate dust particles from *D. montana* (DM) bark, they were rinsed with deionized water and dried in the shade. Separately, 20 g of dried bark was ground and placed in a 500 mL deionized water beaker. For 15 minutes, the aqueous solution was heated till it turned brown. After complete extraction, the brown mixture was allowed to cool to room temperature; it was then filtered using a Whatman No. 1 filter paper and centrifuged for 5 minutes at 1500rpm²⁴. A portion of the crude extract was suspended in water and qualitatively screened for phytochemicals to determine the presence of bioactive components²⁵.

Quantitative Phytochemical Screening

Total Phenol Content

The phenolic content of the DM bark extract was estimated with the help of a UV-Vis spectrophotometer (Shimadzu UV-1900i) method with phenol reagent (Folin and Ciocalteu's) at an absorbance of 725 nm²⁶. Gallic acid was compared to phenolic compounds, and the results are stated as mg of gallic acid equivalents per mg of DM bark extract (mg Gallic acid equivalent/g).

Total Flavonoid Content

The aluminium chloride method was used to determine the flavonoid content of DM bark extract at an absorbance of 510 nm. The flavonoids in the aqueous extract were calculated to be the same as quercetin (g/mg). The result is expressed as mg of quercetin equivalents per gram of DM bark extract (mg Quercetin /g) as a reference flavonoid component for comparison²⁷.

Total Tannin Contents

The tannin concentration of DM bark extract was estimated by the method of Price and Butler with various modifications. A 3.0 mL sample, 3.0 mL vanillin (4 percent) in methanol, and 1.5 mL con. HCl was combined and incubated for 10 minutes in the dark. The tannin content of the samples was then determined using a UV Spectrophotometer set at 500 nm. Results are

presented as mg Catechin /g equivalent²⁸.

Synthesis of *Diospyros montana* Selenium nanoparticles (DM-SeNPs)

For fabrication of DM-SeNPs, a 300 mM selenious acid solution was prepared and agitated for 10 minutes. An aqueous DM bark extract of 10mL was added dropwise with steady stirring. Then 2 mL of 400 mM ascorbic acid was added to help the reduction reaction start. The mixture was incubated at room temperature for 24 hours. The noticeable change in the reaction mixture's colour signified the synthesis's completion. UV spectroscopy was utilized to investigate the reaction mixture at the during the incubation period. A centrifuge (Remi C-854/8) was used to centrifuge the reaction mixture for 20 minutes at 35,00 rpm. When the reaction finished, the pellet was treated with deionized water and ethanol before being dried overnight. The PBS (pH 7.4) was added and centrifuged with ultrasonication for suspending red DM-SeNPs. The powdered product was maintained at 4-5°C and used for subsequent analysis^{23, 29}.

Characterization of DM-SeNPs

The bio-reduction of selenious acid by DM bark extract was monitored using the colour of the reaction mixture. After synthesising the brick-red selenium nanoparticles, the absorbance was determined at wavelengths ranging from 200 to 600 nm using a UV spectrophotometer (Shimadzu UV-1900i). The FT-IR spectra of DM bark extract and DM-SeNPs were determined at wavelengths ranging from 4000–600 cm⁻¹; numerous reducing and stabilizing functional groups of DM aqueous bark extract were identified, as well as their involvement in the production of DM-SeNPs, utilizing a Jasco FT/IR-4600 spectrometer linked to a single ATR accessory (Jasco ATR PRO ONE). XRD (Model-D8 Advanced, BRUKER., and Germany) analysis was used to assess the crystallinity of the DM-SeNPs. SEM analysis was carried out to investigate the shape, surface topology, and morphology of the produced DM-SeNPs. EDAX determined the elemental composition of DM-SeNPs. A scanning electron microscope (Jeol 6390LA) was equipped with an EDX Detector OXFORD XMXN apparatus.

The purity and elemental composition of the sample were determined using the atom percentage of metal in the EDAX analysis. The

size distribution and average diameter of the DM-SeNPs were determined using DLS and zeta potential measurements. The size distribution of DM-SeNPs was determined using a Zetasizer Nano Series (Malvern Pananalytical Ltd., Malvern, UK). The hydrodynamic size of particles was determined using DLS by focussing monochromatic light on the solution, causing a Doppler shift. A wavelength shift occurs when a laser beam strike moving particles and scatters the light at an angle. Scattering light angle is inversely related to particle size. Zeta potential was measured to calculate the surface charge of the DM-SeNPs. ICP-AES (SPECTRO ARCOS, Germany) was used to determine selenium levels at the ppm-level qualitatively. A calibration curve for known selenium was created using a standard (Se) solution at 242.80 nm, and the selenium concentration of DM-SeNPs was calculated. Three replicate experiments were carried out, and the mean (ppm) standard deviation was determined.

Antioxidant Activity

DPPH radical scavenging activity

The DPPH free radical scavenging capability of DM bark extract, DM-SeNPs, Selenium (Se), and Standard Ascorbic acid (AA) was tested at concentrations of 10 to 100 µg/mL. To each 1 mL of the test solution, 2 mL of DPPH reagent was added and incubated in the dark for 10 minutes. The absorbance at 517 nm was determined using a UV spectrophotometer (Shimadzu UV-1900i). The reaction mixture was left without DM-SeNPs as a control, and ascorbic acid was utilized as a positive control^{30,31}. The free radical scavenger activity of DPPH was computed using the method below:

$$\% \text{ RSA} = [(A - B) / A] \times 100,$$

Where A is the absorbance of the DPPH and B is the absorbance of DM-SeNPs

Reducing power activity

The various concentrations (0.2, 0.4, 0.6, 0.8, 1.0 µg/mL) of DM bark extract, DM-SeNPs, Se, and standard AA were analyzed by reducing Fe³⁺ to Fe²⁺ ions. For the reducing power assay, the absorbance was measured at 700 nm using a UV-Vis spectrophotometer (Shimadzu UV-1900i), and ascorbic acid was used as a positive control^{32,33}.

Antibacterial Activity

The well diffusion technique was used

to access the antibacterial activity. This study utilized two Gram-positive bacterial strains (*Bacillus subtilis* and *Staphylococcus aureus*) and two Gram-negative bacterial strains (*Escherichia coli* and *Klebsiella pneumoniae*). Bacterial strains were acquired from the CSIR-Institute of Microbial Technology's Microbial Type Culture Collection (MTCC) and Gene Bank in Chandigarh, India. Muller Hinton agar was produced, sanitized, and aseptically transferred to Petri plates. The media Petri plates were allowed to set and then placed in an incubator overnight to ensure that they were free of contamination. After that, test organisms were inoculated onto the Petri plates, and wells were bored for loading test samples³⁴. To determine antibacterial susceptibility, each well was treated with 20µg/mL and 40µg/mL dose of DM-SeNPs, a positive Control (Ciprofloxacin 1mg/mL), and a negative Control as Dimethyl sulfoxide (DMSO)³⁵. The Hi-media scale was used to quantify inhibitory zones after 24 hours of incubation at 37°C. All experiments were replicated three times, and the mean and standard deviation was calculated.

Antiproliferative Activity

The 3-[4,5-dimethylthiazol-2-yl]-2,5 diphenyl tetrazolium bromide (MTT) assay was performed to determine the antiproliferative activity of DM bark extract, DM-SeNPs, Se, and Doxorubicin as the Control Drug. NCCS, Pune, India, provided the Human Breast cancer cell line (MCF-7). The cells were grown in Dulbecco's Modified Eagle Medium (DMEM) high glucose medium supplemented with 10% FBS and 1% antibiotic-antimycotic solution in a CO₂ incubator at a temperature of 37°C and sub-cultured every two days. The MTT test was used to investigate the proliferation and cytotoxicity of DM-SeNPs. Cell growth and cytotoxic activities were determined using a colorimetric test. This test is based on reducing the yellow-coloured tetrazolium dye MTT to formazan crystals in water. This generates a purple colour upon solubilization in a suitable solvent; the intensity of the colour is related to the quantity of live cells, which may be determined spectrophotometrically at 570 nm³⁶⁻³⁸. Without the test agent, cell culture plates were seeded with 200µL cell suspension at the appropriate cell density on a 96-well plate (20,000 cells per well). After that, cells were allowed to grow for 24 hours. Plates were loaded with appropriate

amounts of DM bark extract (DM), DM-SeNPs, and standard doxorubicin. For 24 hours, the plates were incubated at 37°C in a 5% CO₂ environment. Following incubation, MTT was added at a final concentration of 0.5 mg/mL of total liquid. The plates were then wrapped in aluminium foil to prevent light exposure and incubated for 3 hours. Subsequently, the MTT reagent was removed, and 100µL DMSO was added. Moderate swirling in a gyratory shaker accelerated the dissolution of MTT formazan crystals and entirely dissolved them. The absorbance was determined using a UV spectrophotometer at reference wavelengths 570 nm and 630 nm. The half-maximal inhibitory concentration (IC₅₀) was determined using a linear regression method.

i.e., $Y = Mx + C$.

Where $Y = 50$, M and C values are derived from the cell viability graph.

RESULTS AND DISCUSSION

Qualitative Phytochemical Screening

The qualitative phytochemical screening of DM bark extract is summarised in table 1. The phytochemical screening specified important active phytomolecules such as tannins, terpenoids, saponins, polyphenols, and flavonoids. The

DM bark extract contains a high concentration of tannins, flavonoids, and phenolics, reducing functional groups^{39, 40}. Several phenolics and flavonoids include numerous hydroxyl (-OH) groups capable of chelating metal ions by forming a stable complex between the multiple hydroxyl (-OH) groups and the carbonyl moiety. These functional groups may aid in the reduction of selenious acid to selenium nanoparticles⁴¹. Biomolecules may function as a biocatalyst during the nanomaterials production process. Thus, using plants in the synthesis process minimizes hazardous chemicals and results in an eco-friendly synthesis of nanoparticles NPs.

Quantitative Phytochemical Screening

D. montana bark extract showed a substantial amount of phenolics, flavonoids, and tannins contents depicted in table 2. These critical phytoconstituents may be a valuable source of reducing and capping agents. The tannin concentration of the extract is high, which aids in stabilizing the metal nanoparticles; due to the tannin compounds, it imparts electron-donating capacity and capping characteristics⁴². The green synthesis of metal nanoparticles by plants via phytochemicals may be a marker of their antioxidant capacity owing to the bioactive molecules that have been accumulated on their surface.

Table 1. Qualitative Phytochemical Screening of *D. montana* bark extract

Phytoconstituents	Test	Conclusion
Alkaloids	Dragendroff's test	+
Flavonoids	Shinoda test	+
Glycosides	Keller-Killiani test	+
Phenolics & Tannins	5% FeCl ₃ Test	++
Saponins	Foam test	++
Steroids & Triterpenoids	Liebermann-Burchard's test/Salkowski reaction	++

+: Present in low concentration; ++: Present in high concentration.

Table 2. Quantitative Phytochemical Screening of *D. montana* bark extract

Sr. No	Phytoconstituents	Content (mg/g)
1.	Total Phenolics contents	132.31±2.81
2.	Total Flavonoid contents	53.17±1.36
3.	Total Tannins contents	65.52±0.39

Results are expressed as mean ± S.D. (n = 3).

Synthesis of *D. montana* Selenium Nanoparticles (DM-SeNPs)

The SeNPs were successfully synthesized from *D. montana* bark extract. Initially, the selenious acid solution was colourless, which turned into ruby red after adding *D. montana* bark extract and ascorbic acid as reaction initiator, as shown in Figure 1. The colour changes to ruby red is due to the synthesis of DM-SeNPs, which

is visually noted after 2 hrs. The ruby-red solution formed due to the excitation of the surface plasmon resonance and indicated the reduction of selenious acid into elemental selenium. At applied synthesis conditions, synthesized nanoparticulate dispersion was constantly stirred for 3 h at 30°C in the dark. After the complete reaction, the pellet was rinsed three times with deionized water and then three times with ethanol before being dried overnight at the optimum temperature in an oven. Synthesized DM-SeNPs were then characterized using UV, FT-IR, SEM, DLS, ZP, XRD, EDX, TEM, and ICP-AES.

UV-Visible Spectroscopic analysis

To determine the kinetic behaviors, DM-SeNPs were characterized using a UV-Vis spectrophotometer (Shimadzu UV -1900i). The synthesized DM-SeNPs were confirmed over a range of 200–800 nm using UV spectroscopy. UV spectroscopy revealed the formation of selenium nanoparticles after adding the selenious acid solution to the *D. montana* extract; it changed the colour of the extract from yellow to slightly red, confirming the formation of selenium nanoparticles. The colour shift indicated the conversion of

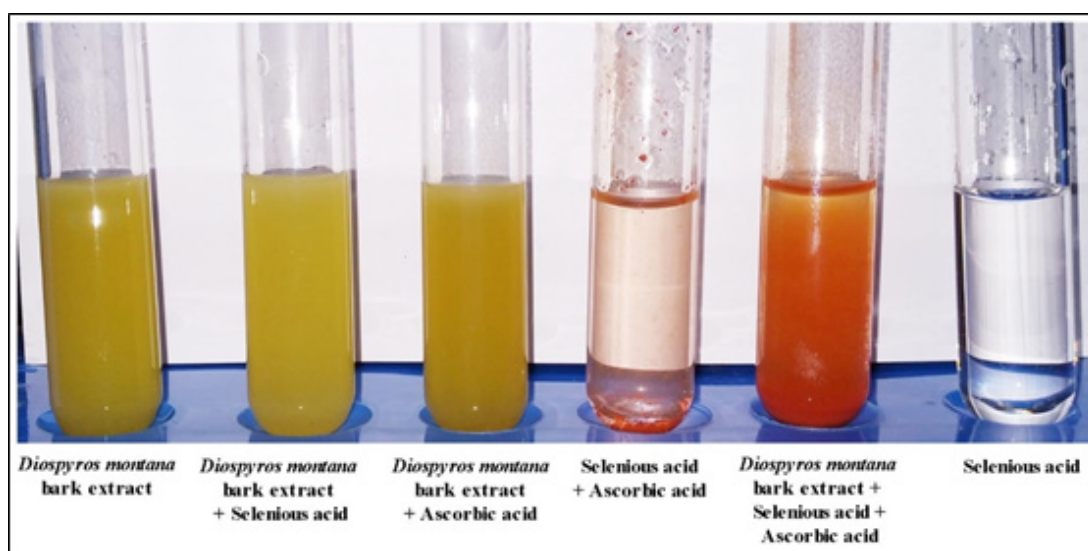


Fig. 1. The visual analysis of the green synthesis of *Diospyros montana* Selenium Nanoparticles

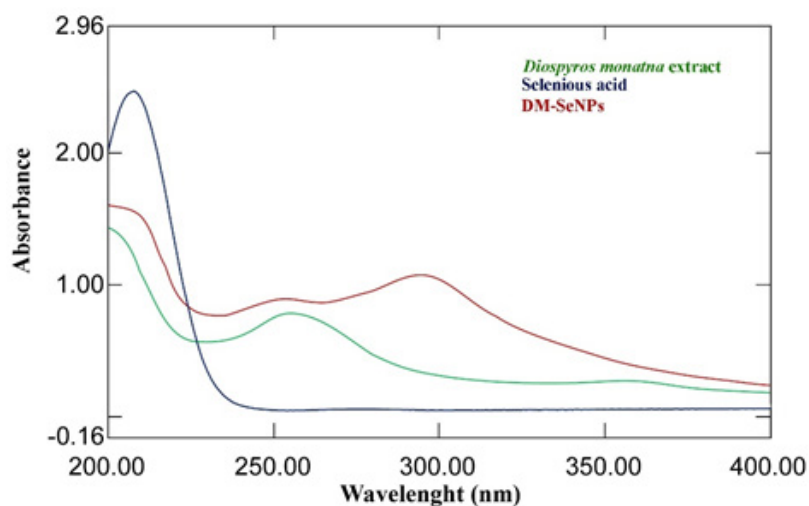


Fig. 2. A) UV-Visible spectra of *Diospyros montana* bark extract and *Diospyros montana* Selenium Nanoparticles and Selenious acid

selenium ions to nano-selenium during the reaction with ascorbic acid. The most readily apparent aspect of nanoparticles is their colour change as they grow in size. Thus, as the size of synthesized particle changes, the particle colour changes display absorption in the visible area of the spectrum, as observed by Angamuthu *et al.*⁴³. The extracts and resultant Se-NPs colour were determined using a UV-Vis spectrophotometer. A band at 255 nm was seen in the aqueous extract of *D. montana* bark. A strong absorbance (ϵ_{max}) at 285 nm confirmed the Synthesis of DM-SeNPs (Figure 2A-B). This absorbance measurement (ϵ_{max}) confirms that the DM-SeNPs were synthesized entirely from *D. montana* bark phytoconstituents. The absence of any other peak in the DM-SeNPs indicated that the synthesized nanoparticles were made entirely of pure selenium.

UV spectroscopy is a function of SeNPs' surface plasmon resonance (SPR). Alhawit A⁴⁴ reported that the Surface Plasmon Resonance (SPR) is owing to the synthesis of SeNPs, which results in a maximal absorption between 200 and 400 nm. The UV spectra were taken at 1, 5, 10, 15, and 30-day intervals following room temperature storage to test the stability of the synthesized DM-SeNPs. The progression of UV spectra is illustrated in Figure 2(B). During the four weeks, there was no discernible change in peak position. The reduction

in intensity reflects a rise in the concentration of Se-NPs and the attainment of the stable absorbance peak. The fact that the absorbance peak remains stable means that no additional particles agglomerate. After 12 days, the significant change in peak maxima and shape is most likely owing to deformation mechanisms such as nanosurface oxidation. These spectra demonstrate that a solution of Se-NPs is stable for about a month.

Fourier transform-infrared spectroscopy (FT-IR) Analysis

The functional groups in DM bark extract were identified using FT-IR spectroscopy. They effectively reduced Se ions to SeNPs and capped the phyto-reduced SeNPs. The FT-IR spectra of DM-SeNPs demonstrate various capping phytomolecules on the surface of the SeNPs, illustrated in Figure 3. In these spectra, the absorption peak at 3291 cm^{-1} has been shifted to 3385 cm^{-1} ; a new peak at 1584 cm^{-1} has been observed in synthesized DM-SeNPs. The peaks at 1687 , 1514 , and 1210 cm^{-1} shifted to 1736 , 1544 , and 1214 cm^{-1} , respectively. Additionally, it established the existence of a unique absorption peak at different wavenumbers in the fingerprint area. e.g., 865 , 733 , 708 , 628 , and 615 cm^{-1} . The shift in the peak position of about $3,400\text{ cm}^{-1}$ shows that selenium nanoparticles were synthesized by reducing the carbonyl groups from DM bark

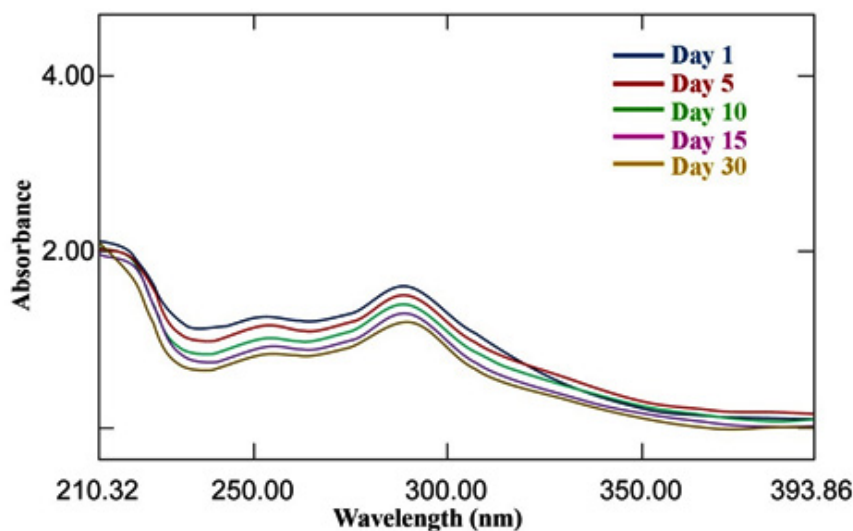


Fig. 2. B) UV-Visible spectra showing the stability of *Diospyros montana* Selenium Nanoparticles

extract. Abhijeet *et al.*⁴⁵ noted similar shifts and development of peaks at 2,922 and 2,965 cm^{-1} , indicating that C-H (SP³ hybridized) and O-H (of acid origin) groups in DM bark extract were involved in particle formation. With an increase in height, the peak at 1,687 cm^{-1} was displaced to

1,736 cm^{-1} . A broad vibration peak in DM-SeNPs at 3385.42 cm^{-1} corresponds to the O-H stretch of alcohols and phenols groups was also reported by Cittrarasu *et al.*⁴⁶. The absorption peak at 2965 and 2916 cm^{-1} is a characteristic of C-H stretch alkynes⁴⁷. The band at 1516 cm^{-1} results from asymmetric

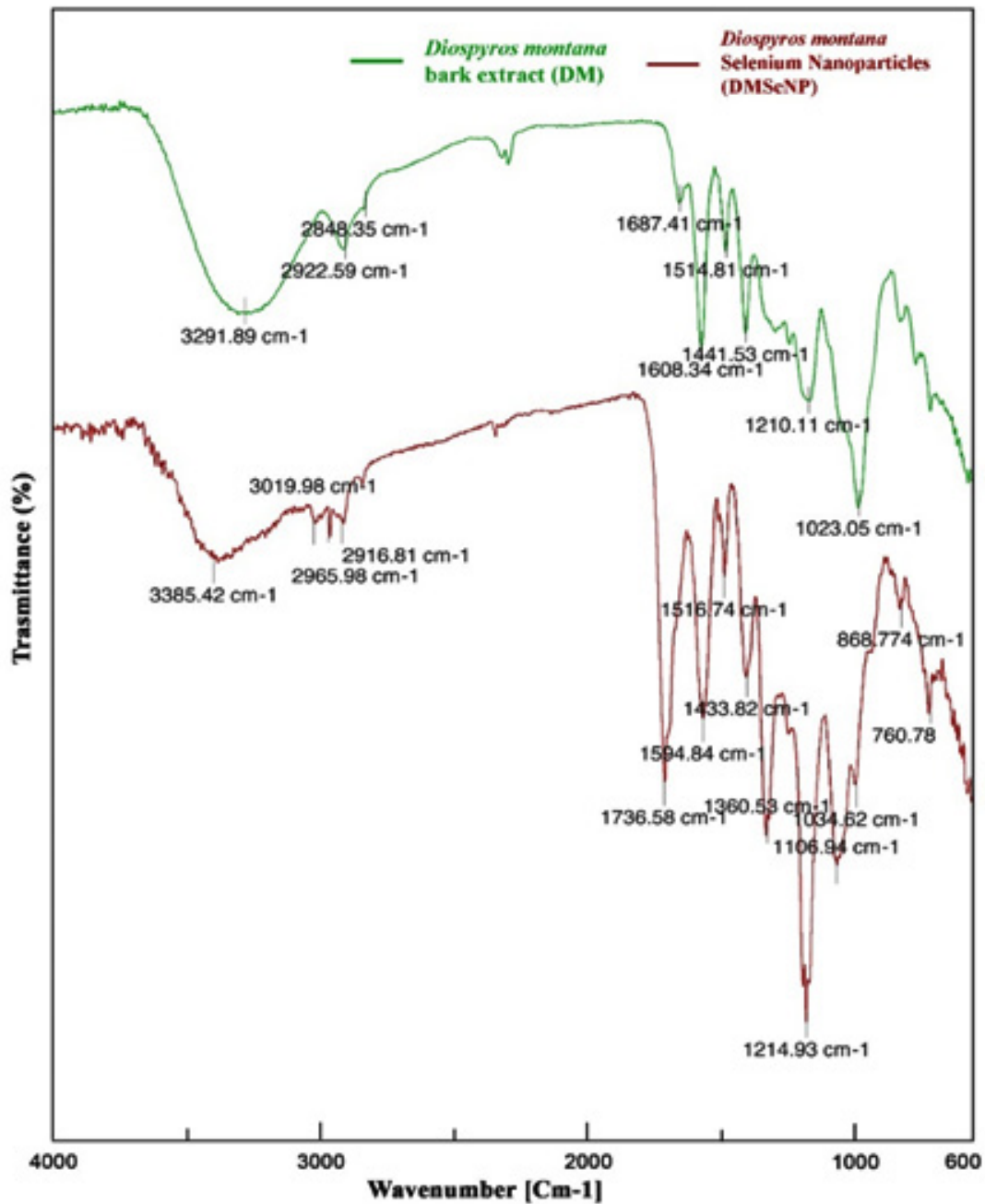


Fig. 3. Fourier transform-infrared Spectrum of *Diospyros montana* bark extract and *Diospyros montana* Selenium Nanoparticles

stretch nitro compounds composed of N-O⁴⁸. The strong band at 1441 cm⁻¹ is due to Alkanes' C-H bending stretching (in the ring) of aromatics. A peak at 1214 cm⁻¹ indicates secondary-OH bending. In the low wavenumber area, a strong band at 1034 cm⁻¹ indicates the superposition of in-plane C-H bending and the distinctive Se-O stretching vibration⁴⁹. At 668 and 465cm⁻¹, further bending vibrations of the Se-O bond are accentuated. The

finding reveals that the phytoextract containing functional groups can assist the process of nanoparticle reduction and stability of the SeNPs⁵⁰.

X-Ray Diffraction (XRD) Analysis

The XRD pattern revealed the amorphous nature of the synthesized DM-SeNPs. The X-ray diffraction pattern is depicted in Figure 4. which indicates that DM-SeNPs are amorphous. The

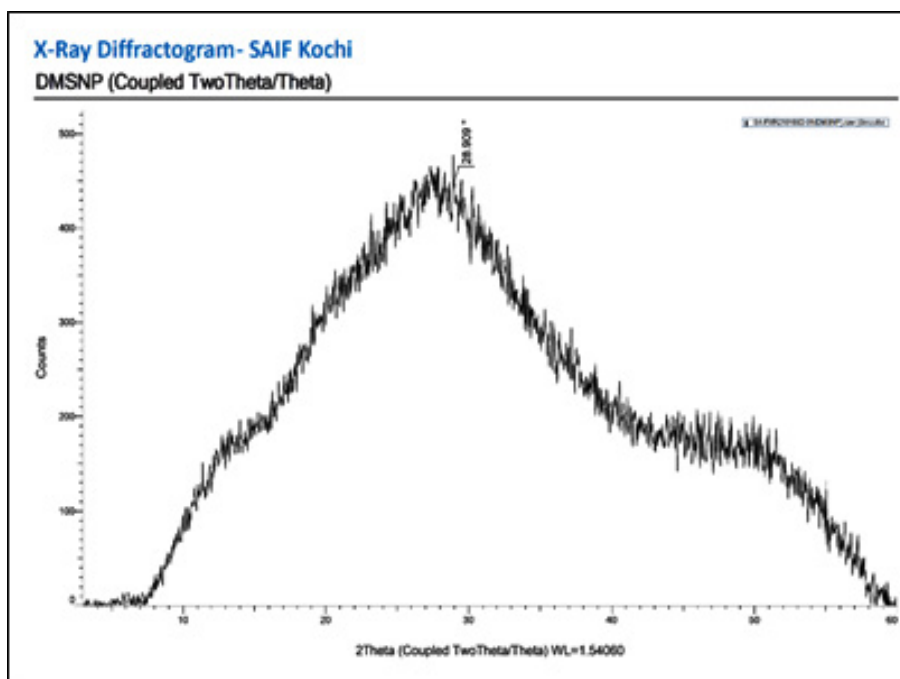


Fig. 4. X-Ray Diffraction pattern of *Diospyros montana* Selenium Nanoparticles

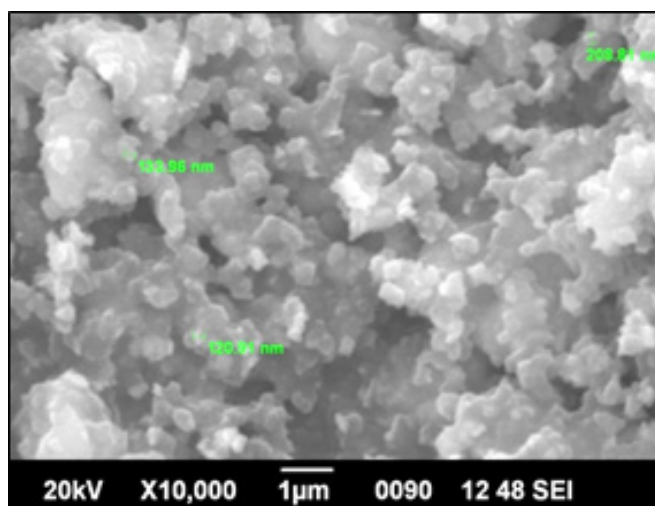


Fig. 5. Scanning Electron Microscopic image indicating the size of *Diospyros montana* Selenium Nanoparticles

X-Ray pattern reveals a broad peak devoid of sharp Bragg's peaks. As a result, it postulates that DM-SeNPs are synthesized in an amorphous state, which refers to the previous reports of Gunti *et al.*⁵¹. The XRD spectrum of DM-SeNPs and their counterparts is identical to that of ordinary selenium powder, confirming the nanoparticle synthesis. The lattice constants calculated are $a = 4.363 \text{ \AA}$ and $c = 4.952 \text{ \AA}$, in accordance with the value derived from the literature (JCPDS File

No.06-0362)^{52,53}. Scherrer's equation was used to determine the crystallite size of DM-SeNPs, which was found to be 140 nm.

Scanning Electron Microscopic Analysis (SEM) Analysis

SEM was used to characterize the morphology of DM-SeNPs synthesized using a green approach shown in Figure 5. SEM photos aided in visualizing the morphology of DM-SeNPs and revealed a spherical shape with a smooth surface

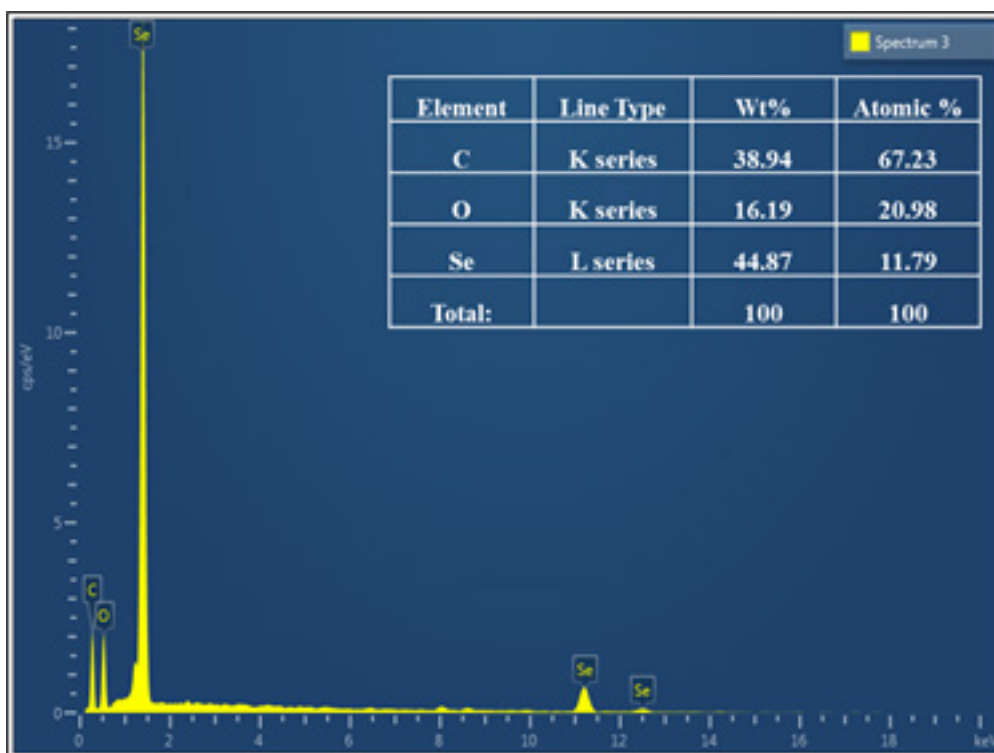


Fig. 6. Energy-Dispersive X-ray Spectrum of *Diospyros montana* Selenium Nanoparticles

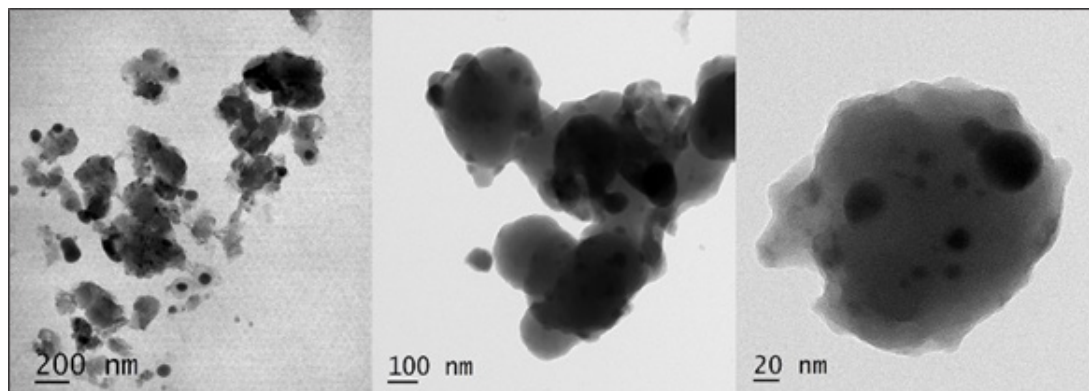


Fig. 7. Transmission Electron Microscopy images of *Diospyros montana* Selenium Nanoparticles

of DM-SeNPs. The particle size of DM-SeNPs was determined to be between 120 and 200 nm when adequately distributed by aggregation. Thus, one may claim that the accretion of nanoparticles triumphs over reduced atoms' reduction and primary nucleation. DM-SeNPs may be associated with more functional groups in *D. montana* bark extract that bind to and nucleate sulfuric acid ions. Minor amounts of the best available metal ions are complex during nucleation, signifying the metal ion's aggregation. Ramamurthy *et al.*⁵⁴ reported that agglomerated nanoparticles exhibit increased biological activity. As a result, biogenic DM-SeNPs may have biological applications.

Energy-Dispersive X-ray Spectroscopy Analysis

EDXA was used to determine the chemical composition of DM-SeNPs. This EDX analysis validated the presence of selenium elemental in the DM-SeNPs sample described in Figure 6. The DM-SeNPs revealed discrete selenium, carbon, and oxygen absorption peaks, with a strong signal from the Selenium (Se) atom (59.59 percent), Oxygen(O) atom (15.56 percent), and Carbon(C) atom (24.84 percent) and absence of any other elemental peak. According to Sharma *et al.*⁵⁵ lack of any other elemental peaks and the high selenium content in the spectrum testifies the purity of the fabricated selenium metal. The DM-SeNPs

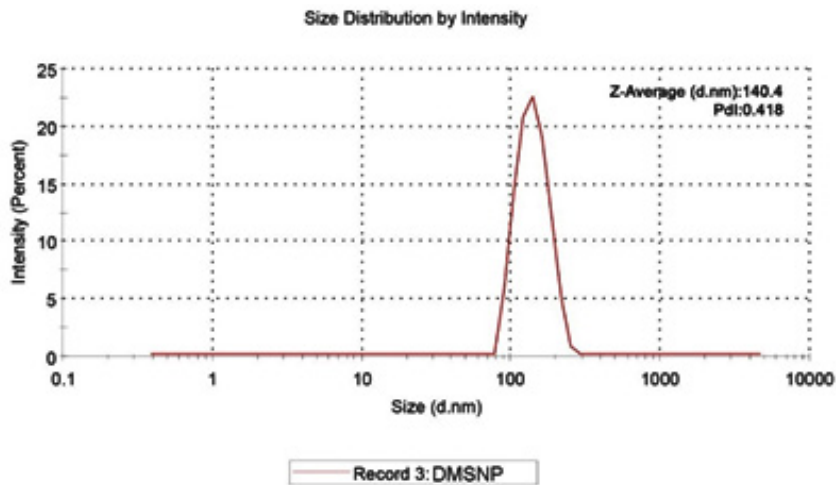


Fig. 8. Dynamic light scattering analysis of *Diospyros montana* Selenium Nanoparticles

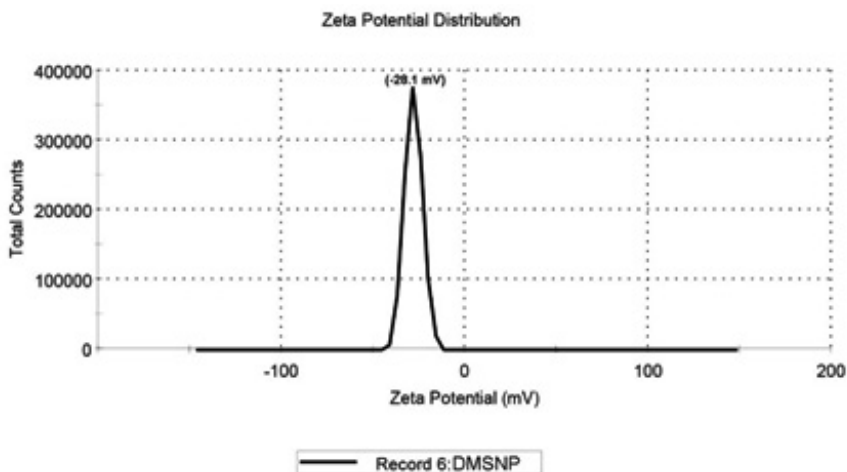


Fig. 9. Zeta potential analysis of *Diospyros montana* Selenium Nanoparticles

spectrum contains oxygen and carbon peaks, indicating the presence of alkyl chain stabilisers.

Transmission Electron Microscopy (TEM)

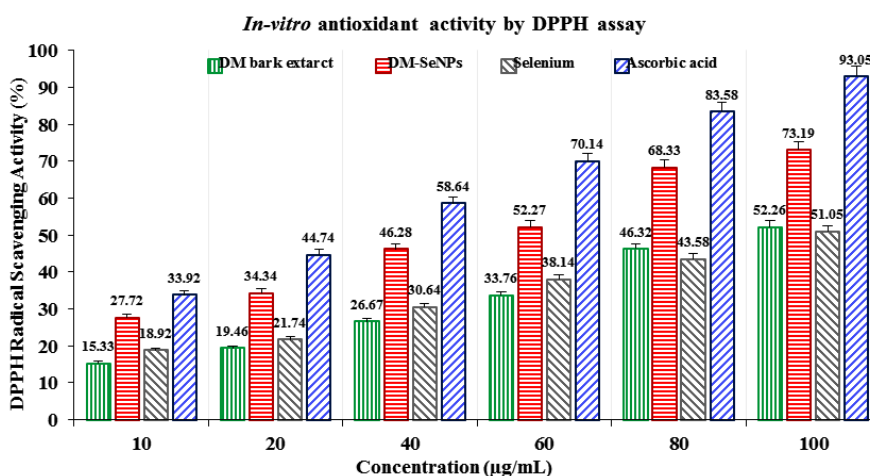
According to TEM with specified area electron diffraction patterns, the DM-SeNPs formed agglomerated particles (amorphous nature). Green synthesized biogenic DM-SeNPs were mono scattering and spherical, as shown in Figure 7. The transmission electron microscopy image confirmed the spherical nature of the DM-SeNPs and their nanoscale size. The DM-SeNPs had a size distribution of 20-200 nm, with an average size of 140 nm. The sizes and forms of the DM-SeNPs synthesized were not reliant on the plant *D.*

montana bark extract utilized in synthesis, which may be attributed to diverse tannins flavonoids and other polyphenolic compounds with reduction potential. Thus, these phytomolecules may drive Se ion reduction to the nanoscale, stabilizing the synthesized DM-SeNPs and prevent their aggregation. The TEM demonstrates a high correlation between the size of the nanoparticles and their biological activity, which is in line with the research of Ahmad and Kalra ⁵⁶.

Size-distribution analysis

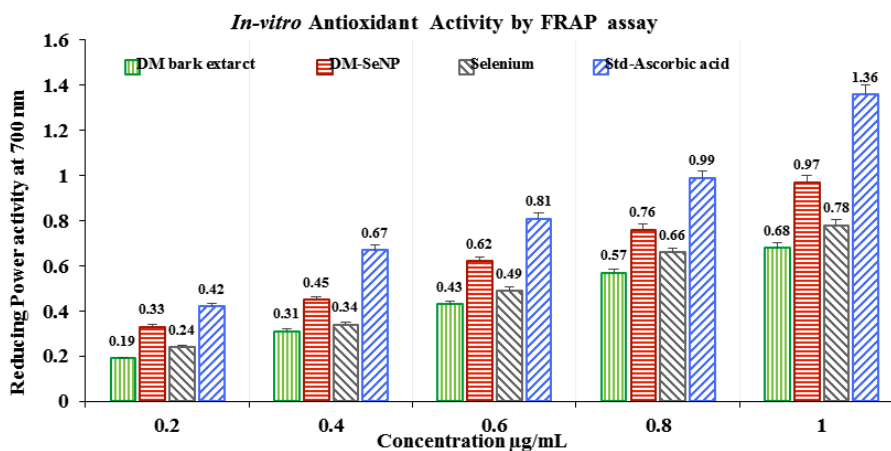
Dynamic Light Scattering (DLS) analysis

Dynamic light scattering (DLS) analysis in an aqueous solution was used to assess the



Results are expressed as mean \pm S.D. (n = 3).

Fig. 10. A) DPPH radical scavenging activity of *Diospyros montana* bark extract, *Diospyros montana* Selenium Nanoparticles, Selenium, and Std-Ascorbic acid



Results are expressed as mean \pm S.D. (n = 3).

Fig. 10. B) Reducing power activity of *Diospyros montana* bark extract, *Diospyros montana* Selenium Nanoparticles, Selenium, and Std-Ascorbic acid

hydrodynamic size and polydispersity index (PDI) of DM-SeNPs. The DLS study depicted in Figure 8 illustrates the particle size distribution of selenium capped/reduced DM-SENPS. The average size of DM-SeNPs was determined to be 140.4 nm, with a polydispersity index (PDI) of 0.418, confirming the homogeneity and uniform dispersion of SeNPs. In practice, TEM and DLS measurements of a particle’s dimensions are different (DLS measurements include the ligand shell and define the hydrodynamic size); nonetheless, DLS and TEM figures are in good agreement with one

another (we can look at the lone metallic core in TEM)⁵⁷. DLS derived size is more significant than the size estimated by TEM images. This is most likely because of the solvation shell generated on the surface of the selenium core by the *D. montana* coat, which contributes to particle diameter only when DLS measurements are conducted, as reported by Zhang *et al.*⁵⁸.

Zeta potential analysis

The zeta potential of DM-SeNPs was determined to be -28.1 mV, shown in Figure 9. This demonstrates the DM-SeNPs’ has great dispersity

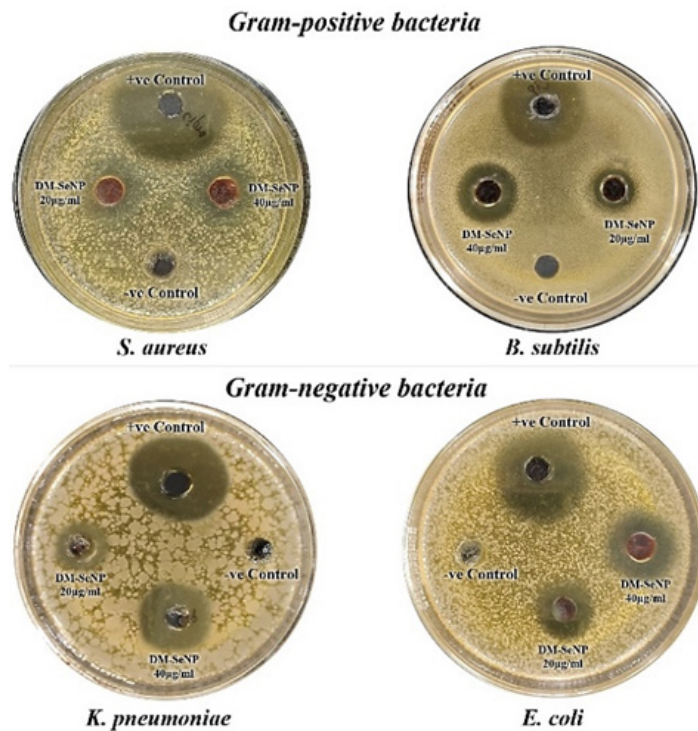


Fig. 11. Antibacterial activity of *Diospyros montana* Selenium Nanoparticles

Table 4. Antibacterial activity of *Diospyros montana* Selenium Nanoparticles (DM-SePs)

Microorganism	Circumference of the zone of inhibition (in mm)			
	DM-SeNP		Positive Control#	Negative Control*
	20µg/mL	40µg/mL		
<i>S. aureus</i>	19.13±0.00	34.16±0.00	89.25±0.00	00.00 ± 0.00
<i>B. subtilis</i>	23.14±0.00	44.14±0.00	83.53±0.00	00.00 ± 0.00
<i>K. pneumoniae</i>	17.42 ± 0.00	36.20 ± 0.00	78.25±0.00	00.00 ± 0.00
<i>E. coli</i>	22.00±0.00	48.00±0.00	72.80±0.00	00.00 ± 0.00

The data represent the mean of triplicates (±) with a standard deviation (mean ±SD; n = 3). # Ciprofloxacin (1 mg/mL) * Dimethyl sulfoxide (DMSO) (25 iL/well)

and stability with negligible aggregation. The zeta potential analysis indicated that the synthesised DM-SeNPs were negatively charged. The negative charge potential was formed due to the reducing agent oxidizing the flavonoid and polyphenolic content of the *D. montana* bark extract. This suggests the presence of large electrostatic forces between the green synthesized DM-SeNPs. Previously, if all particles in a suspension had a negative or positive zeta potential, they tended to reject one another, resulting in a dramatic

reduction in the particles' desire to aggregate. The high stability of DM-SeNPs without aggregation may result from the selenium particles' negative charge⁵⁹.

ICP-AES- Selenium content estimation

ICP-AES was employed to assess the concentration of Selenium in DM-SeNPs. The calibration curve was created using selenium standards ranging from 0.1 to 100 mg/mL. At ppm levels, the calibration curve for selenium was linear, with a correlation coefficient of 0.999.

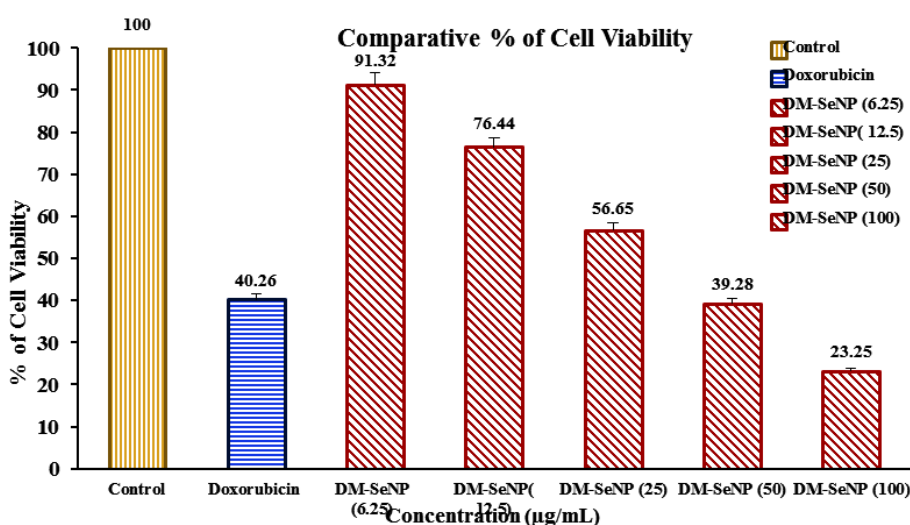


Fig. 12. A) Percentage of cell viability of Control, Standard Doxorubicin, and *Diospyros montana* Selenium Nanoparticles treated MCF7 cells

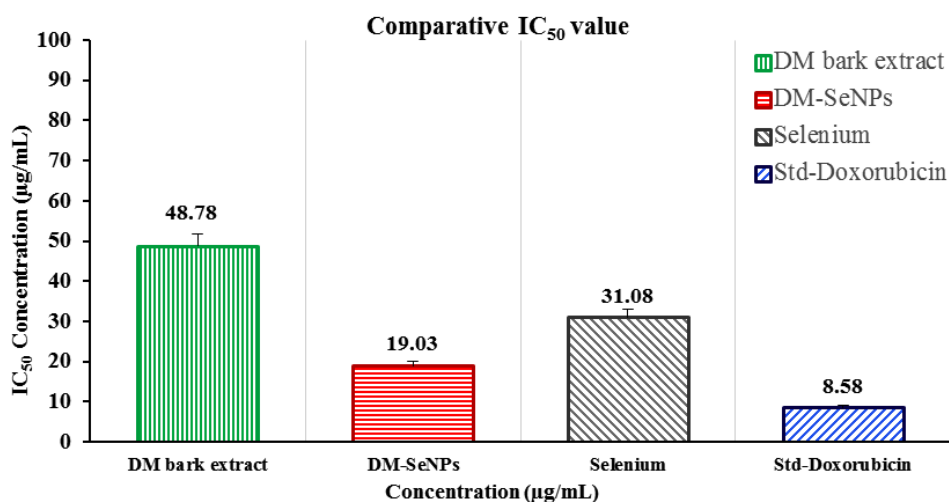


Fig. 12. B) Comparative IC₅₀ values of *Diospyros montana* bark extract, *Diospyros montana* Selenium Nanoparticles, Selenium, and Std-Doxorubicin

Following nitric acid treatment, the samples discolored, indicating that the selenium had been dissolved in solution. ICP-AES investigation found a selenium content of $63.45 \pm 18.3 \mu\text{g/mL}$ in DM-SeNPs.

Antioxidant Activity of DM-SeNPs

The DPPH assay was used to assess the free radical scavenging activities of the *D. montana* aqueous extract, DM-SeNP, Selenium Se, and Standard ascorbic acid. The capacity of DM-SeNPs to scavenge free radicals was determined spectrophotometrically by the change in the intensity of the DPPH colour from purple to yellow. The proportion of DPPH scavenging activity increased as the concentrations of all solutions increased (10-100 ppm). At a $100 \mu\text{g/mL}$ concentration, DM-SeNPs demonstrated 76.43 percent scavenging action, compared to selenium at 51.05 percent and *D. montana* bark aqueous extract at 46.26 percent, respectively, and standard ascorbic acid at 93.15 percent (Figure 10A). The studies show that antioxidant activity is size and concentration-dependent when IC_{50} values of DM-SeNPs $24.72 \pm 0.63 \mu\text{g/mL}$, Selenium $41.63 \pm 0.25 \mu\text{g/mL}$, *D. montana* aqueous extract $74.42 \pm 0.33 \mu\text{g/mL}$, and standard (ascorbic acid) at $12.51 \pm 0.16 \mu\text{g/mL}$ are compared. The antioxidant potential of the DM-SeNPs was much greater than that of the *D. montana* extract and was comparable

to that of standard ascorbic acid. Reduction capacity was highly correlated with antioxidant capacity and is likely to be a key antioxidant attribute. According to the reducing capacity of each sample used in the reducing power assay, the test solution changes colour from yellow to different hues of green and blue. In this case, a remarkable reduction in capacity was observed as concentration increased. Standard (ascorbic acid) and DM-SeNPs have EC_{50} values of $28.46 \pm 34 \mu\text{g/mL}$ and $46.30 \pm 0.21 \mu\text{g/mL}$, respectively (Figure 10B). The DM-SeNPs demonstrated a considerably free radical scavenging activity compared to normal ascorbic acid. These findings indicate that DM-SeNPs function as an effective radical scavenger. Free radicals produced in-vivo act as signaling and regulatory molecules during normal cellular metabolism.

On the other hand, excessive free radicals cause damage to cellular molecules, ultimately impairing their normal function. Numerous publications propose novel biological potential for SeNPs as antioxidants, owing primarily to their redox modulatory properties⁶⁰. Several investigations have suggested that amorphous SeNPs have exceptional antioxidant potential⁶¹.

Antibacterial Activity of DM-SeNPs

The antibacterial properties of DM-SeNPs were evaluated against four pathogenic bacterial

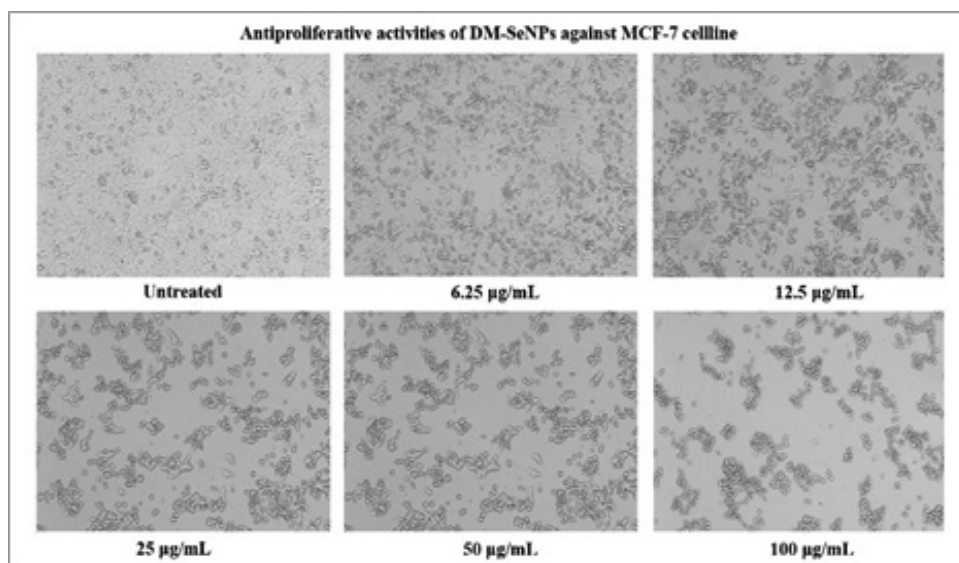


Fig. 12. C) Antiproliferative activities of *Diospyros montana* Selenium Nanoparticles against human breast cancer cell lines (MCF-7) at various concentrations (6.25-100 $\mu\text{g/mL}$)

strains: *Escherichia coli* (*E. coli*) (MTCC 10312), *Klebsiella pneumoniae* (*K. pneumoniae*) (MTCC 3040), *Staphylococcus aureus* (*S. aureus*) (MTCC 1144), and *Bacillus subtilis* (*B. subtilis*) (MTCC 1144). Ciprofloxacin was utilized as a positive control, whereas DMSO was employed as a negative control, as shown in table 4. DM-SeNPs were shown to be effective against all pathogens. The inhibitory zones were found to be the highest zone for *E. coli* (48.00 mm), *B. subtilis* (44.14 mm), *Klebsiella pneumoniae* (36.20 mm), and *S. aureus* (34.16mm), respectively, as indicated in Figure 11. While ciprofloxacin exhibited the most significant inhibition zone, DM-SeNPs exhibited an inhibition zone equivalent to ciprofloxacin. DM-SeNPs exhibit a more excellent zone of inhibition against *B. subtilis* and *E. coli*, implying that they may be used as an antimicrobial agent.

Antiproliferative Activity of DM-SeNPs

The statistical analysis of cell cytotoxicity data using MTT against MCF-7 suggests that the test compounds, namely DM-SeNPs, Se, and Standard Doxorubicin, have substantially greater cytotoxic potential than DM. As demonstrated in Figure 12. (A-B-C) DM bark extract had minimal proliferative inhibition on MCF-7; Se showed a minute antiproliferative activity toward MCF-7, whereas DM-SeNPs exerted potential antiproliferative activity toward MCF-7 cells in comparison to Standard Doxorubicin. The IC_{50} values for DM $65.35 \pm 0.21 \mu\text{g/mL}$, DM-SeNPs $38.19 \pm 0.27 \mu\text{g/mL}$, SeNPs $21.77 \pm 0.33 \mu\text{g/mL}$, and Standard Doxorubicin. $6.41 \pm 0.09 \mu\text{g/mL}$, respectively, suggest that DM and SeNPs display moderate cytotoxicity, whereas DM-SeNPs demonstrate high cytotoxicity (Figure 12 B). The Microscopic cell morphological observation discovered a uniform intracellular distribution of DM-SeNPs in cancer cells. DM-SeNPs treated cells displayed chromosome instability and mitotic apprehension in cancer cells (MCF-7). The antiproliferative activity was measured by significant inhibition of the growth of MCF-7 cells on treatment with DM-SeNPs, as shown in Figure 12C. Microscopic cell morphological observation after MTT staining showed that cells treated with DM-SeNPs reduced cell viability, loss of cell-to-cell contact, cell shrinkage, and formation of apoptotic bodies. The antiproliferative effect could be a result of well-characterized DM-SeNPs. This

paper proposes a novel method for synthesizing DM-SeNPs with antitumor potential. The same principle would apply to additional SeNPs, contributing to developing SeNPs-mediated drug carriers. Metallic nanoparticles synthesized from plant extracts exhibit increased tumor selectivity, promising efficacy, and negligible toxicity to healthy cells. The cytotoxic effect of nanoparticles mainly results from their enormous surface area, which permits efficient drug administration, and specific nanoparticles display anticancer activity⁶².

CONCLUSION

Biogenic synthesis of selenium nanoparticles is successful since the biomolecules used in the reduction process are derived from plants and are thus entirely non-toxic to the environment. The significant discovery of this study was the identification of tannins, flavonoids, and phenolics, all of which were determined to be suitable for the biosynthesis of SeNP. FTIR proves that biosynthesized DM-SeNPs are stable due to the capping of these phytoconstituents. The characterization results showed DM-SeNPs were stable, had a negative charge, were amorphous, had a spherical form, and were nanoscale in size. The XRD spectra established the amorphous nature of DM-SeNPs with characteristic selenium absorption spectra. The EDAX analysis confirmed the elemental composition of DM-SeNPs. Additional TEM and particle size distribution measurements validated the spherical shape of DM-SeNPs. The spherical amorphous DM-SeNPs demonstrated significant antioxidant activity as measured by DPPH scavenging and reducing power capacity assays. DM-SeNPs exhibit a more excellent zone of inhibition against *B. subtilis* and *E. coli*, indicating that they might be employed as an antibacterial agent. Hence DM-SeNPs can be a potential antibacterial agent in treating bacteria-related disorders. The MTT assays investigated the antiproliferative activity on MCF-7 cell lines; it demonstrated that DM-SeNPs possess substantial cytotoxic potential in a dose-dependent manner compared to doxorubicin; hence it may be employed as an anticancer agent. This study indicates that DM-SeNPs have a high degree of growth control compared to cancer cells, indicating their

potential for medicinal applications. In the future, combining phytomolecules and nanoparticles may play a significant role in treating several disorders. Thus, it offers novel opportunities to formulate and develop well-fabricated biogenic SeNPs that may be manufactured, stored, and commercialized safely worldwide.

ACKNOWLEDGEMENTS

The authors acknowledge the Indian Institute of Technology Bombay, Mumbai, Sophisticated test and instrumentation center, Cochin, Pinnacle Biomedical Research Institute, Bhopal, and SNJB College of Pharmacy, Chandwad, Maharashtra, for their instrumental technical support. The authors would also like to express gratitude to Dr. (Mrs.) Savita J. Tauro, Principal, St. John Institute of Pharmacy and Research, Palghar, for the generous support and necessary facilities to carry out this research work.

Conflict of interest

The authors declare no conflict of interest, financial or otherwise.

Funding source

The research was supported by the University of Mumbai APD/ICD/2019-20/762 [Project No: Pharmacy/Sr. No.-516]

REFERENCES

- Baig N, Kammakam I, Falath W. Nanomaterials: A review of synthesis methods, properties, recent progress, and challenges. *Materials Advances*. 2021;**2**(6):1821-71.
- Khan I, Saeed K, Khan I. Nanoparticles: Properties, applications and toxicities. *Arabian Journal of Chemistry*. 2019;**12**(7):908-31.
- Murthy SK. Nanoparticles in modern medicine: state of the art and future challenges. *Int J Nanomedicine*. 2007;**2**(2):129-41.
- Rai M, Nagaonkar D, P. Ingle A. Metal nanoparticles as therapeutic agents: A Paradigm shift in medicine. *Metal Nanoparticles* 2018. p. 33-48.
- Patra JK, Das G, Fraceto LF, Campos EVR, Rodriguez-Torres MdP, Acosta-Torres LS, et al. Nano based drug delivery systems: recent developments and future prospects. *Journal of Nanobiotechnology*. 2018;**16**(1):71.
- Diallo MS, Fromer NA, Jhon MS. Nanotechnology for sustainable development: retrospective and outlook. *Journal of Nanoparticle Research*. 2013;**15**(11):2044.
- Gour A, Jain NK. Advances in green synthesis of nanoparticles. *Artificial Cells, Nanomedicine, and Biotechnology*. 2019;**47**(1):844-51.
- Menon S, K.S SD, Agarwal H, Shanmugam VK. Efficacy of biogenic selenium nanoparticles from an extract of Ginger towards evaluation on Antimicrobial and Anti-Oxidant activities. *Colloid and Interface Science Communications*. 2019;**29**:1-8.
- Abhijeet P, Swati P, Mandar M. Biomedical applications of biogenic phytonanoparticles: A review. *International Journal of Botany Studies*. 2021;**6**(3):534-40.
- Bhattacharjee A, Basu A, Bhattacharya S. Selenium nanoparticles are less toxic than inorganic and organic selenium to mice in vivo. *The Nucleus*. 2019;**62**(3):259-68.
- Sakr TM, Korany M, Katti KV. Selenium nanomaterials in biomedicine-An overview of new opportunities in nanomedicine of selenium. *Journal of Drug Delivery Science and Technology*. 2018;**46**:223-33.
- Hariharan S, Dharmaraj S. Selenium and selenoproteins: it's role in regulation of inflammation. *Inflammopharmacology*. 2020;**28**(3):667-95.
- Ansar S, Alshehri SM, Abudawood M, Hamed SS, Ahamad T. Antioxidant and hepatoprotective role of selenium against silver nanoparticles. *Int J Nanomedicine*. 2017;**12**:7789-97.
- Bai K, Hong B, Huang W, He J. Selenium-Nanoparticles-Loaded Chitosan/Chitooligosaccharide Microparticles and Their Antioxidant Potential: A Chemical and In Vivo Investigation. *Pharmaceutics*. 2020;**12**(1):43.
- Shoeibi S, Mozdziak P, Golkar-Narenji A. Biogenesis of selenium nanoparticles using green chemistry. *Topics in Current Chemistry*. 2017;**375**(6):88.
- Pyrzynska K, Sentkowska A. Biosynthesis of selenium nanoparticles using plant extracts. *Journal of Nanostructure in Chemistry*. 2021.
- Zambonino MC, Quizhpe EM, Jaramillo FE, Rahman A, Santiago Vispo N, Jeffryes C, et al. Green Synthesis of Selenium and Tellurium Nanoparticles: Current Trends, Biological Properties and Biomedical Applications. *International Journal of Molecular Sciences*. 2021;**22**(3):989.
- Ghaffari-Moghaddam M, Hadi-Dabanlou R, Khajeh M, Rakhshanipour M, Shameli K. Green synthesis of silver nanoparticles using plant extracts. *Korean Journal of Chemical Engineering*. 2014;**31**(4):548-57.
- Ebbo A, Mammam M, Suleiman M, Ahmed A,

- Bello A. Preliminary phytochemical screening of *Diospyros mespiliformis*. *Anatomy & Physiology: Current Research*. 2014;**4**(4):156-8.
20. Kantamreddi V, Wright CW. Investigation of Indian *Diospyros* species for antiplasmodial properties. *Evidence-based Complementary and Alternative Medicine*. 2008;**5**(2):187-90.
21. Tanwar AK, Sharma R, Gupta SK. Methanolic fraction from Tamala (*Diospyros montana* Roxb.) ameliorates anxiety like behaviour via 5-HT_{2A} pathway in rats. *Phytomedicine Plus*. 2022;**2**(1):100150.
22. Bharathi D, Diviya Josebin M, Vasantharaj S, Bhuvaneshwari V. Biosynthesis of silver nanoparticles using stem bark extracts of *Diospyros montana* and their antioxidant and antibacterial activities. *Journal of Nanostructure in Chemistry*. 2018;**8**(1):83-92.
23. Kokila K, Elavarasan N, Sujatha V. *Diospyros montana* leaf extract-mediated synthesis of selenium nanoparticles and their biological applications. *New Journal of Chemistry*. 2017;**41**(15):7481-90.
24. Amiri H, Hashemy SI, Sabouri Z, Javid H, Darroudi M. Green synthesized selenium nanoparticles for ovarian cancer cell apoptosis. *Research on Chemical Intermediates*. 2021.
25. Puri AV. Quantitative phytochemical screening, thin-layer chromatography analysis, high-performance thin-layer chromatography fingerprinting, and antioxidant activity of leaves of *Diospyros montana* (Roxb.). *Asian Journal of Pharmaceutical and Clinical Research*. 2019;**12**(2):325-31.
26. Adebisi OE, Olayemi FO, Ning-Hua T, Guang-Zhi Z. In vitro antioxidant activity, total phenolic and flavonoid contents of ethanol extract of stem and leaf of *Grewia carpinifolia*. *Beni-Suef University Journal of Basic and Applied Sciences*. 2017;**6**(1):10-4.
27. Yin K, Ismail A, Mohamed M, Kwei Y. *Euphorbia hirta* methanolic extract displays potential antioxidant activity for the development of local natural products. *Pharmacognosy Research*. 2019;**11**(1).
28. Arya A, Aditya, Nyamathulla, Shaik, Noordin, Noordin MI, et al. Antioxidant and Hypoglycemic activities of leaf extracts of three popular *Terminalia* Species. *E-Journal of Chemistry*. 2012;**9**(2):883-92.
29. Dhawan G, Singh I, Dhawan U, Kumar P. Synthesis and Characterization of Nanoselenium: A Step-by-Step Guide for Undergraduate Students. *Journal of Chemical Education*. 2021;**98**(9):2982-9.
30. El-Zayat MM, Eraqi MM, Alrefai H, El-Khateeb AY, Ibrahim MA, Aljohani HM, et al. The Antimicrobial, Antioxidant, and Anticancer activity of green synthesized selenium and zinc composite nanoparticles using *Ephedra aphylla* extract. *Biomolecules*. 2021;**11**(3):470.
31. Kumar V, Sharma N, Sourirajan A, Khosla PK, Dev K. Comparative evaluation of antimicrobial and antioxidant potential of ethanolic extract and its fractions of bark and leaves of *Terminalia arjuna* from north-western Himalayas, India. *J Tradit Complement Med*. 2017;**8**(1):100-6.
32. Irshad M, Zafaryab M, Singh M, Rizvi MMA. Comparative Analysis of the Antioxidant Activity of *Cassia fistula* Extracts. *International journal of medicinal chemistry*. 2012;**2012**:157125-.
33. Chatha SAS. Bioactive components and antioxidant Properties of *Terminalia arjuna* L. extracts. *Journal of Food Processing & Technology*. 2014;**05**(2):298.
34. Jadhav K, Dhamecha D, Dalvi B, Patil M. Green synthesis of silver nanoparticles using *Salacia chinensis*: Characterization and its Antibacterial activity. *Particulate Science and Technology*. 2015;**33**(5):445-55.
35. Alagesan V, Venugopal S. Green synthesis of selenium nanoparticle using leaves extract of *Withania Somnifera* and its biological applications and photocatalytic activities. *BioNanoScience*. 2019;**9**(1):105-16.
36. Alley MC, Scudiero DA, Monks A, Hursey ML, Czerwinski MJ, Fine DL, et al. Feasibility of Drug Screening with Panels of Human Tumor Cell Lines Using a Microculture Tetrazolium Assay. *Cancer Research*. 1988;**48**(3):589.
37. Mosmann T. Rapid colorimetric assay for cellular growth and survival: Application to proliferation and cytotoxicity assays. *Journal of Immunological Methods*. 1983;**65**(1):55-63.
38. Gerlier D, Thomasset N. Use of MTT colorimetric assay to measure cell activation. *Journal of Immunological Methods*. 1986;**94**(1):57-63.
39. Mandal S, Patra A, Samanta A, Roy S, Mandal A, Mahapatra TD, et al. Analysis of phytochemical profile of *Terminalia arjuna* bark extract with antioxidative and antimicrobial properties. *Asian Pac J Trop Biomed*. 2013;**3**(12):960-6.
40. Saha A, Pawar VM, Jayaraman S. Characterisation of Polyphenols in *Terminalia arjuna* Bark Extract. *Indian J Pharm Sci*. 2012;**74**(4):339-47.
41. Kirupakaran R, Saritha A, Bhuvaneshwari S. Green synthesis of selenium nanoparticles from leaf and stem extract of *Leucas lavandulifolia* Sm. and their Application. *Journal of Nanoscience and Technology*. 2016;**2**(5): 224-6.
42. Koopmann A-K, Schuster C, Torres-Rodríguez J, Kain S, Pertl-Obermeyer H, Petutschnigg

- A, et al. Tannin-Based hybrid Materials and their applications: A Review. *Molecules*. 2020;**25**(21):4910.
43. Angamuthu A, Venkidusamy K, Muthuswami RR. Synthesis and Characterization of Nano-selenium and its Antibacterial Response on Some Important Human Pathogens. *Current Science*. 2019.
44. Alhawiti AS. Citric acid-mediated green synthesis of selenium nanoparticles: antioxidant, antimicrobial, and anticoagulant potential applications. *Biomass Conversion and Biorefinery*. 2022.
45. Abhijeet P, Swati P. *Tinospora cordifolia* stem extract-mediated green synthesis of selenium nanoparticles and its biological applications. *Pharmacognosy Research*. 2022;**14**(3):1-7.
46. Cittrarasu V, Kaliannan D, Dharman K, Maluventhen V, Easwaran M, Liu WC, et al. Green synthesis of selenium nanoparticles mediated from *Ceropegia bulbosa* Roxb extract and its cytotoxicity, antimicrobial, mosquitocidal and photocatalytic activities. *Scientific Reports*. 2021;**11**(1):1032.
47. Tugarova AV, Mamchenkova PV, Dyatlova YA, Kamnev AA. FTIR and Raman spectroscopic studies of selenium nanoparticles synthesised by the bacterium *Azospirillum thioophilum*. *Spectrochimica Acta Part A: Molecular and Biomolecular Spectroscopy*. 2018;**192**:458-63.
48. ElSaied BEF, Diab AM, Tayel AA, Alghuthaymi MA, Moussa SH. Potent antibacterial action of phyco-synthesized selenium nanoparticles using *Spirulina platensis* extract. *Green Processing and Synthesis*. 2021;**10**(1):49-60.
49. Kannan S, Mohanraj K, Prabhu K, Barathan S, Sivakumar G. Synthesis of selenium nanorods with assistance of biomolecule. *Bulletin of Materials Science*. 2014;**37**:1631-5.
50. Prasad KS, Selvaraj K. Biogenic Synthesis of Selenium Nanoparticles and Their Effect on As(III)-Induced Toxicity on Human Lymphocytes. *Biological Trace Element Research*. 2014;**157**(3):275-83.
51. Gunti L, Dass RS, Kalagatur NK. Phytofabrication of selenium nanoparticles from *Emblica officinalis* fruit extract and exploring Its Biopotential Applications: Antioxidant, Antimicrobial, and Biocompatibility. *Frontiers in Microbiology*. 2019;**10**.
52. Dwivedi C, Shah CP, Singh K, Kumar M, Bajaj PN. An Organic Acid-induced Synthesis and Characterization of Selenium Nanoparticles. *Journal of Nanotechnology*. 2011;**2011**:651971.
53. Shah CP, Singh KK, Kumar M, Bajaj PN. Vinyl monomers-induced synthesis of polyvinyl alcohol-stabilized selenium nanoparticles. *Materials Research Bulletin*. 2010;**45**(1):56-62.
54. Ramamurthy CH, Sampath KS, Arunkumar P, Kumar MS, Sujatha V, Premkumar K, et al. Green synthesis and characterization of selenium nanoparticles and its augmented cytotoxicity with doxorubicin on cancer cells. *Bioprocess and Biosystems Engineering*. 2013;**36**(8):1131-9.
55. Sharma G, Sharma AR, Bhavesh R, Park J, Ganbold B, Nam J-S, et al. Biomolecule-Mediated synthesis of selenium nanoparticles using dried *Vitis vinifera* (Raisin) extract. *Molecules*. 2014;**19**(3):2761-70.
56. Ahmad W, Kalra D. Green synthesis, characterization and anti microbial activities of ZnO nanoparticles using *Euphorbia hirta* leaf extract. *Journal of King Saud University - Science*. 2020;**32**(4):2358-64.
57. Kasture MB, Patel P, Prabhune AA, Ramana CV, Kulkarni AA, Prasad BLV. Synthesis of silver nanoparticles by sophorolipids: Effect of temperature and sophorolipid structure on the size of particles. *Journal of Chemical Sciences*. 2008;**120**(6):515-20.
58. Zhang W, Zhang J, Ding D, Zhang L, Muehlmann LA, Deng S-e, et al. Synthesis and antioxidant properties of Lycium barbarum polysaccharides capped selenium nanoparticles using tea extract. *Artificial Cells, Nanomedicine, and Biotechnology*. 2018;**46**(7):1463-70.
59. Sajadi SM, Nasrollahzadeh M, Maham M. Aqueous extract from seeds of *Silybum marianum* L. as a green material for preparation of the Cu/Fe₃O₄ nanoparticles: A magnetically recoverable and reusable catalyst for the reduction of nitroarenes. *Journal of Colloid and Interface Science*. 2016;**469**:93-8.
60. Khurana A, Tekula S, Saifi MA, Venkatesh P, Godugu C. Therapeutic applications of selenium nanoparticles. *Biomedicine & Pharmacotherapy*. 2019;**111**:802-12.
61. Li Y, Li X, Wong YS, Chen T, Zhang H, Liu C, et al. The reversal of cisplatin-induced nephrotoxicity by selenium nanoparticles functionalized with 11-mercapto-1-undecanol by inhibition of ROS-mediated apoptosis. *Biomaterials*. 2011;**32**(34):9068-76.
62. Rao PV, Nallappan D, Madhavi K, Rahman S, Jun Wei L, Gan SH. Phytochemicals and biogenic metallic nanoparticles as Anticancer agents. *Oxidative Medicine and Cellular Longevity*. 2016;**2016**:3685671.